Multicomponent Electrodes for Water Oxidation: From Combinatorial to Individual Electrode Study

Alexandre G. Dokoutchaev, Feras Abdelrazzaq, and Mark E. Thompson*

Department of Chemistry, University of Southern California, Los Angeles, California 90089

Jennifer Willson, Clark Chang, and Andrew Bocarsly*

Department of Chemistry, Princeton University, Princeton, New Jersey 08544

Received December 20, 2001. Revised Manuscript Received May 15, 2002

Combinatorial screening of platinum group metal (PGM) microelectrodes supported on graphite paper was carried out in a search for useful electrodes for water oxidation. This screening utilized a fluorescent acid−base indicator to identify the most active electrodes in 10 × 10 arrays. Individual Pt, Pd, Ir, Ru, Os, and Rh samples and mixtures of these metals were used to investigate their activities as electrodes for water oxidation. Supported Ru was the most active (i.e., had the lowest overpotential for water oxidation), but it was unstable when the applied potential was more than 1 V. A mixture of Ru and Ir showed significantly improved stability and activity for water oxidation. The most effective electrodes were composed of the four metals Ru, Pd, Ir, and Pt in a 47:15:23:15 atomic percent ratio. Bulk electrodes were also prepared for Pt/Pd mixtures by a sol−gel method. The optimal ratio of Pt to Pd found in the supported electrodes gave the highest activity for the bulk electrodes as well.

Introduction

Nanoparticulate platinum group metals (PGMs) exhibit useful catalytic properties and are widely used as microelectrodes in chemical reactions, such as photochemical water decomposition,[1] hydrogen peroxide production,[2] fuel cell reactions,[3] and the decomposition of nitrogen oxides and other pollutants in automobile exhaust.[4] With the development of new combinatorial screening methods,[5] it has become possible to study a large number of different metal combinations as catalysts in parallel. In recent studies, it was found that aggregates composed of three or even four metals have much higher electrode activities than mono- or bimetallic electrodes for methanol oxidation.[5,6]

The design of simple, inexpensive, and effective systems for photochemical water decomposition[7] is an important goal. Many systems have been reported to work successfully using ultraviolet radiation,[8−10] but there is still a need to design systems capable of effectively using visible light to split water.[11] The main difficulty in using solar energy to produce hydrogen and oxygen directly from water is the comparatively low energy of visible photons[12] (∼2−3 eV) relative to the 1.23 V needed to dissociate water into hydrogen and oxygen. Unfortunately, conventional electrodes have a significant overpotential for water oxidation, making the voltage required for splitting water higher than the thermodynamic value. To use photon energy in a more effective manner, this overpotential must be reduced to a low level, which is usually achieved by using supported metal nanoparticles (microelectrodes), such as ruthenium oxide or platinum.[7,13,14] Lowering the overpotential for water oxidation and reduction would also be very valuable in fuel cells, leading to higher available cell voltages.

Mallouk et al. recently reported a combinatorial screening method for surveying electrochemical processes.[5,6] In this method, a pH-sensitive fluorescent indicator dye was used to screen a variety of anode materials for methanol oxidation. Their electrode arrays, or libraries, were prepared on graphite paper supports. Each electrode in the library was a different mixture of platinum group metals (PGMs), prepared by the deposition of mixtures of the PGM salts, followed by $NaBH_4$ reduction. The libraries were then used to

* To whom correspondence should be addressed. M.E.T.: met@usc.edu. A.B.B.: bocarsly@chemvax.princeton.edu.

(1) *Energy Resources through Photochemistry and Catalysis*; Gratzel, M., Ed.; Academic Press: New York, 1983.
(2) Dokoutchaev, A.; Krishnan, V. V.; Thompson, M. E.; Balasubramanian, M. *J. Mol. Structe.* **1998**, *470*, 191.
(3) Arico, A. S.; Monforte, G.; Modica, E.; Antonucci, P. L.; Antonucci, V. *Electrochem. Commun.* **2000**, *2* (7), 466.
(4) Akama, H.; Matsushita, K. *Catal. Surv. Jpn.* **1999**, *3* (2), 139.
(5) Reddington, E.; Sapienza, A.; Gurau, B.; Viswanathan, R.; Sarangapani, S.; Smotkin, E.; Mallouk, T. *Science* **1998**, *280*, 1735.
(6) Gurau, B.; Viswanathan, R.; Liu, R.; Lafrenz, T. J.; Ley, K. L.; Smotkin, E. S.; Reddington, E.; Sapienza, A.; Chan, B. C.; Mallouk T. E. *J. Phys. Chem. B* **1998**, *102*, 9997.
(7) Amouyal, E. *Solar Energy Mater. Solar Cells* **1995**, *38*, 249.
(8) Domen, K.; Kudo, A.; Onishi, T. *J. Catal.* **1986**, *102*, 92.
(9) Inoue, Y.; Kubokawa, T.; Sato, K. *J. Phys. Chem.* **1991**, *95*, 4059.
(10) Kiwi, J.; Gratzel, M. *J. Phys. Chem.* **1986**, *90* (4), 637.
(11) Licheng, S.; Brglund, H.; Davydov, R.; Norrby, T.; Hammastrom; Korall, P.; Borje, A.; Philouze, C.; Berg, K.; Tran, A.; Andersson, M.; Stenhagen, G.; Martensson, J.; Almgren; M.; Styring, S.; Akermark, B. *J. Am. Chem. Soc.* **1997**, *119*, 6996.
(12) Lewis, N. S. *Am. Sci.* **1995**, *83*, 534.
(13) Sayama, K.; Arakawa, H. *J. Chem. Soc., Faraday Trans.* **1997**, *93* (8), 1647.
(14) Ogura, S.; Kohno, M.; Sato, K.; Inoue. Y. *Appl. Surf. Sci.* **1997**, *121/122*, 521.

10.1021/cm0117230 CCC: $22.00
Published on Web 06/25/2002

oxidize an aqueous solution containing CH_3OH, electrolyte, and a pH-sensitive fluorescent dye, adjusted to near neutral pH. The oxidation of methanol, eq 1, leads to the release of protons near the anode. The fluorescent dye chosen exhibits strong fluorescence at low pH and is completely quenched at moderate to neutral pH. The dye will thus fluoresce strongly in the vicinity of active electrodes and not emit near inactive electrodes or in any other parts of the cell. By gradually increasing the potential applied to the library of electrodes and monitoring the electrodes that exhibit fluorescence first, it was possible for Mallouk et al. to identify the electrodes with the lowest overpotentials for methanol oxidation.

$$CH_3OH + H_2O \rightarrow CO_2 + 6H^+ + 6e^- \qquad (1)$$

In the present article, we discuss the application of combinatorial screening to the optimization of catalysts for water oxidation, eq 2. In our search for the most effective metal microelectrode for water oxidation, we describe here the detailed study of a variety of supported metal electrodes prepared from combinations of Pt, Pd, Ir, Ru, Os, and Rh.

$$2H_2O \rightarrow 4H^+ + O_2 + 4e^- \qquad (2)$$

Methods

Toray carbon paper (TCP, Toray, Inc.) was used for the preparation of PGM nanoaggregate libraries. To remove any oil residue from the TCP surface, pieces of calculated area were ultrasonically cleaned in water/methanol/acetone (1:1:1 by volume) mixtures for 15 min and then rinsed with acetone and air-dried.

The following PGM salts were used as purchased: $PdCl_2$, $OsCl_3$, $RhCl_3$, $RuCl_3$, H_2PtCl_6 (Aldrich), and $IrCl_3$ (Strem Chemicals). To slow the hydrolysis process and facilitate the solubility of the chloride salts, the pH of the solutions was adjusted to 2 with hydrochloric acid.

Preparation of Combinatorial Libraries. Stock solutions (5×10^{-4} M) of the PGM salts were prepared in 90:10 (by volume) mixture of water and 2-propanol. The supported PGM electrodes were prepared by first depositing the appropriate PGM solution(s) as small droplets (total volume = 10 μL or more) onto the surface of the cleaned TCP. After air-drying, the TCP-supported electrodes were calcined in air and reduced in an atmosphere of 5% H_2 in nitrogen at 430 °C (4 h for calcination and 4 h for reduction). The presence of metal nanoparticles on the surface of TCP was confirmed by SEM/EDX analysis. The multielement libraries were initially prepared in $10\%_{atom}$ steps (i.e., $M1_{0.9}M2_{0.1}$, $M1_{0.8}M2_{0.2}$, $M1_{0.7}M2_{0.3}$, etc.) and tested to estimate the best range of compositions for more detailed study. The optimal composition was then determined with libraries prepared in $4\%_{atom}$ steps.

Fluorescence Screening. For the screening of large PGM arrays of different compositions, a technique previously described by Mallouk was used.[5] PTP (3-pyridin-2-yl-<4,5,6>-triazolo-<1,5-a>pyridine) fluorescent indicator was prepared in our laboratory according to a procedure described earlier.[5,15] Indicator solution (200 mL) containing PTP (100 μM), $Ni(ClO_4)_2$ (30 mM), and $NaClO_4$ (0.5 M) was prepared immediately before the experiment, and the pH was gradually adjusted by $HClO_4$ addition to the point where fluorescence occurs. Subsequently, 0.05 mL of a 0.1 M NaOH solution was added to neutralize the excess of H^+. Resulting solution was weakly acidic with a pH of ~3.

Electrochemical Experiments. The catalysts were tested by measuring current as a function of potential using a PAR model 283 potentiostat/galvanostat. A 2 × 1 cm piece of carbon paper containing a spot of PGM aggregates was used as the working electrode, Pt wire as the counter electrode, and SCE as the reference. The working electrode was immersed in electrolyte solution such that the same area (1 × 1 cm) of conductive surface/electrolyte contact was ensured and any contact between electrolyte and the electrical contact to the TCP support was avoided. The voltage was scanned from 0 to 1.4 V at a rate of 5 mV/s. Electrochemical studies were performed in 0.5 M $NaNO_3$ in deionized water (pH = 5.6, Millipore Milli-RX20 system).

Bulk Electrode Preparation. Bulk metal electrodes were prepared from cyanogels using sol−gel processing. The cyanogels were made by reacting 10 mL of 0.09 M aqueous solution of Na_2PdCl_4 with 5 mL of a 0.09 M aqueous solution of $K_2Pt(CN)_4$. The resulting orange gel was aged for 24 h at room temperature and then dried to the xerogel in a 100 °C oven for 24 h. The xerogel was then sintered in a quartz tube inserted into a furnace under an argon atmosphere for 5 h at 600 °C. *Warning: The possibility exists that either cyanogen or hydrogen cyanide gas might be evolved. Therefore, it is essential to trap the furnace gases with a series of bubblers containing aqueous solutions of sodium hydroxide and bleach.*

X-ray powder diffraction analyses were performed on Rigaku Miniflex X-ray powder diffractometer using Cu Kα radiation. Samples were scanned from a glass background at 1.2°/min. Electron microprobe (EMPA) data were collected using a CAMECA SX-50 instrument. High-spectral-resolution X-ray measurements were made using crystal monochromators and gas flow X-ray detectors. Analyses were performed using an accelerating current of 15 kV and a regulated beam current of 20 nA. Both secondary and backscattered electrons were used to locate areas suitable for analysis. The spatial resolution for a point analysis was approximately 1 mm^3 for the instrument conditions reported above.

Results and Discussion

Supported PGM electrodes were prepared by deposition of small droplets (10 μL) of dilute (5×10^{-4} M) aqueous solution of PGM salts. After complete drying overnight at room temperature, calcination and reduction were carried out at 430 °C. The area of carbon paper covered by the PGM electrodes was typically 2 mm in diameter. It was difficult to differentiate the PGM-treated regions of the carbon paper from the untreated regions by the naked eye. The PGM-coated regions were clearly discernible by scanning electron microscopy (SEM).

SEM/EDX studies were performed to determine the size, morphology, and composition of the PGM nanoparticles formed on the TCP surface. The average size of the nanoaggregates obtained after calcination or calcination/reduction procedures was found to be roughly 20−25 nm (see Figure 1). This size is near the resolution limit of the SEM instrument used here, making any size comparison for different PGMs and their combinations impossible. The PGM particles appeared to be distributed homogeneously on the graphite paper.

Semiquantitative EDX analysis was used to identify the PGM nanoaggregates and estimate the compositions of large individual particles or agglomerates of small particles (50−100 nm). The supported nanoparticles consistently had the same PGM ratio, which was close to the ratio of PGM ions deposited on the surface. Although this suggests that the nanoparticles are an alloy of the PGMs deposited rather than a mixture of nanoparticles of individual metals, we cannot exclude the latter possibility because of the resolution constraints of our SEM instrument.

(15) Mori, H.; Sakamoto, S.; Mashito, S.; Matsuoka, Y.; Matsubashi, M.; Sakai, K. *Chem. Pharm. Bull.* **1993**, *41*, 1944.

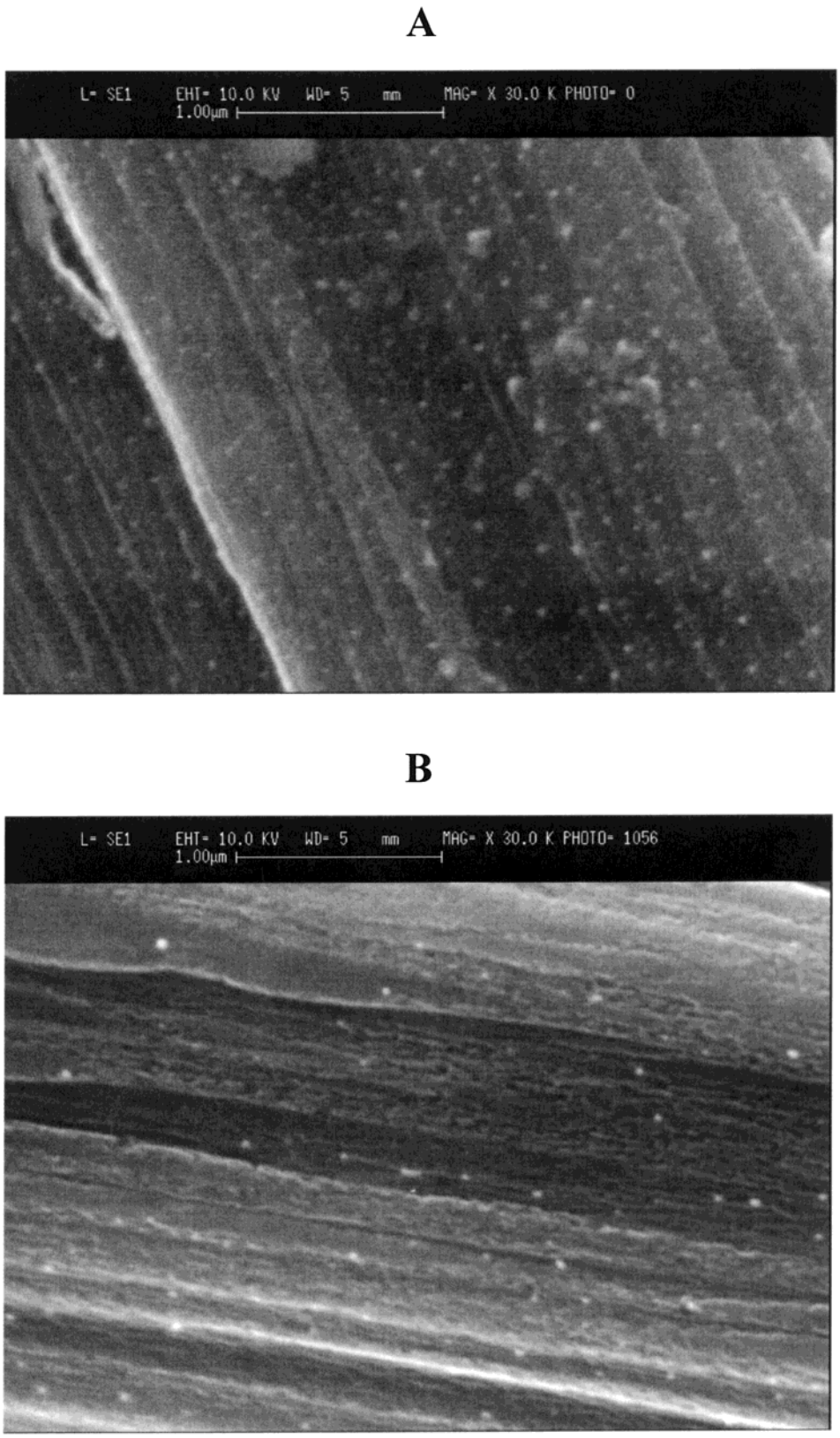

Figure 1. SEM micrographs of TCP-supported nanoaggregates of (A) Pd and (B) Pt.

Electrodes used in combinatorial screening as well as individual testing were prepared under identical conditions. In combinatorial screening arrays, catalytic spots were situated in square matrix with a 5-mm distance between centers, so the total size of the combinatorial library was roughly 65 × 65 mm. Individual TCP electrodes had working areas 10 × 10 mm with the catalytic spot situated in the center of this space.

The initial fluorescence screening method for supported PGM libraries is similar to that reported for screening methanol oxidation catalysts.[5] Similarly to methanol oxidation, water oxidation generates protons,

which lower the pH in the vicinity of the electrode. The key to this screening method is the pH-sensitive fluorescent dye dissolved in the electrolyte solution. The dye fluoresces strongly at acidic pH's and is quenched at neutral or basic pH's; thus, it is possible to screen for active electrodes by monitoring fluorescence. For the system examined here, the precision of visual screening for dye fluorescence is limited, and only coarse optimization of PGM alloys for water oxidation can be achieved. Coarse narrowing of libraries of potential electrode materials was very useful and was carried out by the fluorescence method. However, analysis of the electrochemical properties of the individual electrodes was the best method for optimizing the composition.

The first electrochemical experiments were carried out with nanoparticulate Pt, Pd, Ru, and Ir and their oxides on TCP supports. Fluorescence screening of electrode activity revealed that the onset of visible fluorescence from these TCP-supported microelecrodes is between 0.7 and 0.8 V. This observation is in good agreement withthe value of $E°$ calculated from the Nernst equation at the conditions of the combinatorial screening experiment (pH = 3), which is 0.62 V vs SCE. Monometallic Pt, Pd, Ru, and Ir aggregates were used to determine whether the hydrogen-reduced nanoparticles perform better than the metal oxide electrodes (calcined only, with no hydrogen reduction step) in the water oxidation reaction. Estimations of the fluorescence intensity by visual observation revealed that the activities of the reduced metal electrodes are much higher than those of supported metal oxide. Judging from this observation, all of our subsequent testing involved reduced metal nanoparticles.

From visual observations of the fluorescence, it was found that the most active mixtures are those containing at least $50\%_{\text{atomic}}$ or more of Ir or Ru. The visibly brightest fluorescence was observed on Ru/Ir (Ru contents from 30 to $100\%_{\text{atom}}$), Ru/ Pd (Ru contents from 70 to $100\%_{\text{atom}}$), and Ir/Pt (Ir contents from 80 to $100\%_{\text{atom}}$) bimetallic aggregates. These observations are qualitative, and variations of the applied potential ramp did not provide a better estimation of the relative catalytic activities of the individual electrodes. For more quantitative studies, the individual supported PGM electrodes were prepared, and their electrochemical properties were studied directly.

To establish a solid baseline for comparison, the six individual metals were examined electrochemically. Figure 2 shows that the activities of supported Ru and Ir electrodes are much higher than those of Pt, Pd, Os, and Rh electrodes. By plotting the $I-V$ curves on log−log scales (see Figure 2B) we can estimate the point where the electrochemical reaction begins as the point where the slope of the $I-V$ curve changes markedly, which will be referred to as the "turn-on voltage". The TCP electrode without PGM aggregates gives the lowest anodic current, i.e., a very high overpotential for water oxidation reaction. Only at relatively high values of applied potential (1.4 V) do the Pt, Pd, Os, and Rh activities differ markedly from that of the TCP electrode. Ru aggregates begin to exhibit considerable electrocatalytic activity at 1 V, but repetitive scans show that increasing the applied potential to values higher that 1.1−1.2 V results in irreversible loss of electrode activity. In the case of Ir, electrochemical current begins to increase at higher values of applied potential (1.15 V), but unlike Ru, Ir exhibits the same activity after several repetitive scans. These observations are in good agreement with data reported by Miles and Thomason.[16] They studied electrocatalytic activities of different metals prepared by mixed Rf sputtering onto glass substrates as anodes and cathodes for water electrolysis and found that, for the oxygen evolution reaction, the order of catalytic activity is Ir ≈ Ru > Pd > Rh > Pt. In our experiments, the order of metals according to their catalytic activity is Ru > Ir > Pd ≈ Pt ≈ Os ≈ Rh.

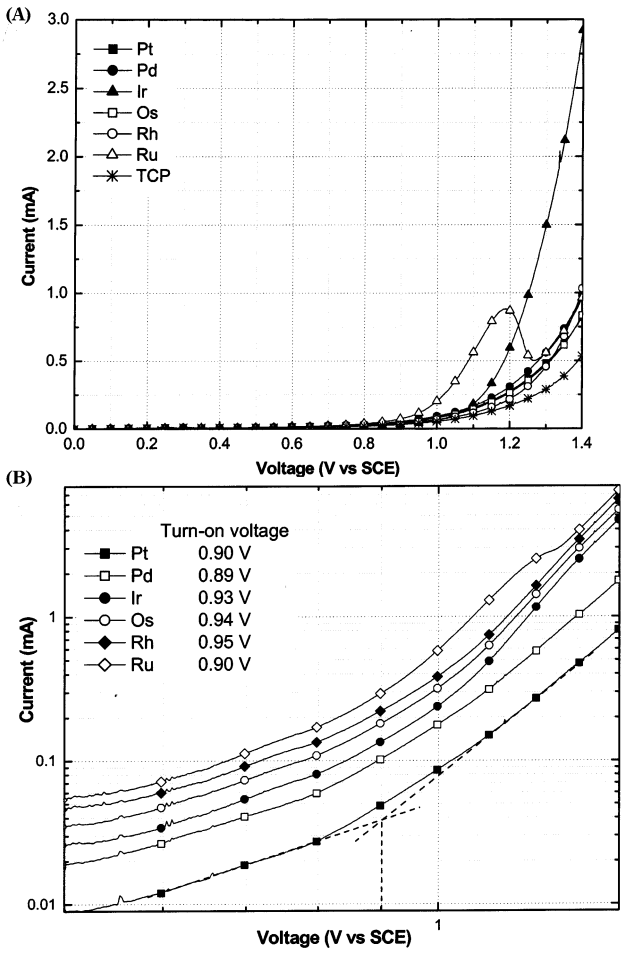

Figure 2. Comparison of catalytic activity of 6 individual PGM nanoaggregates. The lowest line indicates the activity of a Toray carbon paper electrode without any metal deposition. Some of these curves are shown on a logarithmic scale in Figure 2B.

Adding a small amount of Ir, Pt, or Pd (see Figure 3) to a Ru electrode significantly improves the stability of that electrode relative to an electrode of Ru alone. In addition, the Ir/Ru mixture exhibits electrocatalytic activity superior to either of the individual metals (Table 1). However, increasing the level of Ir addition beyond $20\%_{\text{atom}}$ reduces the activity (Table 1). Although Pt and Pd do enhance the stability of the Ru electrode, the amounts required are much higher for Pt or Pd than for Ir, this leading to mixtures that have poorer activities than Ru alone.

(16) Miles, M. H.; Thomason, M. A. *J. Electrochem. Soc.* **1976**, *123* (10), 1459.

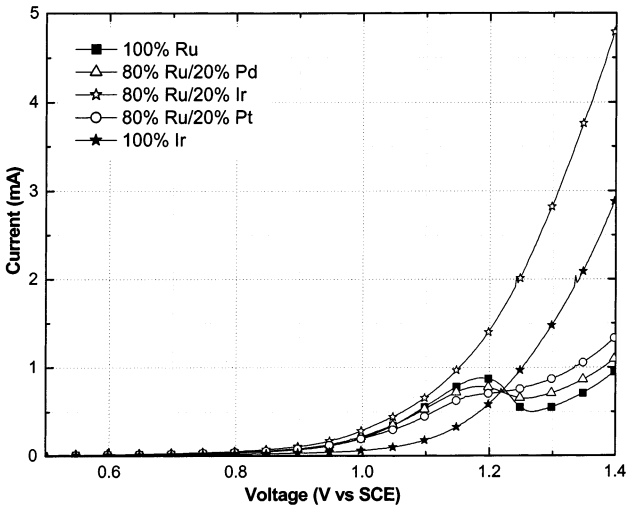

Figure 3. Results of doping of Ru by 20%$_{atom}$ of Ir, Pt, or Pd.

Table 1. Values of Current[a] at Different Applied Potentials Obtained from Tests of Pure PGM Microelectrodes and Some of the Most Representative Combinations

electrode Ru/Pt/Ir/Pd[b]	applied potential (V)			
	1.0	1.1	1.2	1.3
carbon paper	0.053	0.095	0.168	0.289
Rh	0.067	0.115	0.216	0.456
Os	0.080	0.143	0.264	0.468
Pt	0.087	0.152	0.274	0.482
Pd	0.093	0.164	0.310	0.56
Ir	0.061	0.181	0.596	1.498
Ru	0.202	0.563	0.870	0.560
80/0/20/0	0.288	0.666	1.420	2.850
60/0/40/0	0.175	0.515	1.249	2.810
52/20/28/0	0.300	0.942	2.200	3.980
44/20/36/0	0.309	0.867	1.990	3.770
47/19/19/15	0.368	1.017	2.240	3.870
47/15/23/15	0.392	1.077	2.420	4.430

[a] In mA. [b] Ru/Pt/Ir/Pd value given in %$_{atomic}$.

These observations agree with those reported by Koetz and Stucki.[17] They investigated the stability of thin-film Ru/Ir alloy anodes for oxygen evolution from acidic solutions (1 N H_2SO_4) and found that even a small addition (14%$_{atom}$) of Ir strongly stabilizes the Ru anode, which otherwise corrodes and dissolves to form RuO_4. This stabilization phenomenon was attributed to the formation of a protective, insoluble mixed oxide layer, "passivating" the surface of Ru. This hypothesis agrees with our observations and strongly supports the formation of alloyed particles rather than mixtures of monometallic aggregates. For the TCP-supported electrodes, the degree of stabilization gradually increases with increasing Ir content. When the Ir content is 50%$_{atom}$, the electrode is as stable as pure Ir, and has a reduced overpotential in comparison with those of the pure metals. However, the overpotential for the most stable electrode was higher than the value obtained with lower percentages of Ir (see Table 1).

Observations made by SEM/EDX analysis can provide qualitative information about the stability and composition of the supported metal electrodes. For the supported Ru electrode, the decrease in catalytic activity at potentials above 1.2 V is most likely caused by oxidation of nanoparticles to more soluble forms of Ru, just as observed for thin films of Ru.[17] The supported Ru electrode shows a significant amount of Ru by EDX anaysis immediately after preparation or after being soaked in electrolyte for an extended period. EDX scans of the supported Ru electrode, after being used for electrochemical water oxidation at 1.2 V, shows that nearly all of the Ru is lost. This observation is unique for the supported samples of Ru alone. SEM analysis of supported electrocatalysts obtained from combinations of Ru and Pt, Pd, or Ir on TCP revealed that the amount of Ru and the other PGM after water oxidation had not significantly changed. In the case of Ir, this stabilizing action was demonstrated at comparatively low Ir concentrations (roughly 10−15%$_{atom}$), whereas the concentrations of Pt or Pd needed for Ru stabilization were much higher (>30%$_{atom}$). This observation of enhanced stability for mixtures of Ru and a second PGM strongly suggests that the supported metals are nanoparticulate alloys, rather than mixtures of separate Ru and PGM particles. If the supported Ru and PGM samples were separate particles, we would expect the Ru particles to be unstable, just as are the samples of Ru alone.

Tests performed on ternary and quaternary mixtures (see Figure 4) show that they are more suitable for water oxidation than binary mixtures. The maximum electrode activity was observed for microelectrodes of composition: 47%$_{atom}$ Ru, 15%$_{atom}$ Pt, 23%$_{atom}$ Ir, and 15%$_{atom}$ Pd. The electrode activity of this mixture is 2−3 times higher than those of individual Ir or Ru electrodes and significantly higher than those of the most active binary combination (Table 1). Interestingly, the activity of these quaternary mixtures is very sensitive to composition and strongly decreases with changing composition (see Table 2). The most active ternary mixture is composed of Ru, Ir, and Pt (see Figure 4). The composition of this mixture is close to the composition of the best four-element mixture, and its activity is only 10−20% lower than the activity of the best Ru/Pt/Ir/Pd electrode. None of the other three PGMs tested have activities comparable to those of electrodes prepared with Ru, Pt, and Ir. For the most active PGM combinations, the turn-on voltages fall closer together than for individual PGMs, at approximately 0.9 V (see Figure 4B).

It is important to verify whether the observations made for highly dispersed forms of the metals on the solid support have any bearing on the metal choices for bulk metal electrodes. To verify the improvement of the catalytic activity of bimetallic bulk electrodes compared to electrodes prepared from individual metals, we synthesized a bulk metal electrode of a Pt/Pd mixture by the sol−gel method (as described earlier) and compared its catalytic activity to that of a pure Pt electrode. XRPD and EPMA characterization of the Pt/Pd alloy gave a Pt/Pd ratio of 1/1.75. Then, the electrode was mounted on a Cu wire and tested in 1 M H_2SO_4 for water oxidation activity (see Figure 5). From Figure 5, we can see a trend of activity for the electrodes made by sol−gel synthesis similar to that observed for electrodes synthesized on TCP.

(17) Koetz, R.; Stucki, S. *J. Electrochem. Soc.* **1985**, *132* (1), 103.

Table 2. Values of Current[a] at Different Applied Potentials Obtained from the Most Active PGM Combination and Some of the Closest Neighbors

V (V)	best	+Pt−Ir	+Pd−Ir	+Pt−Ru	+Ru−Ir	+Ir−Ru	+Pd−Ru	+Ir−Pd	+Ir−Pt
Ru/Pt/ Ir/Pd[b]	47/15/ 23/15	47/19/ 19/15	47/15/ 19/19	43/19/ 23/15	51/15/ 19/15	43/15/ 27/15	43/15/ 23/19	47/15/ 27/11	47/11/ 27/15
1	0.392	0.368	0.324	0.231	0.261	0.198	0.207	0.351	0.372
1.1	1.077	1.017	0.863	0.695	0.804	0.62	0.662	0.97	1.047
1.2	2.42	2.24	1.92	1.722	2.02	1.53	1.688	2.245	2.36
1.3	4.43	3.87	3.42	3.3	3.88	3.01	3.33	3.955	4.185

[a] In mA. [b] Ru/Pt/Ir/Pd value given in $\%_{atomic}$.

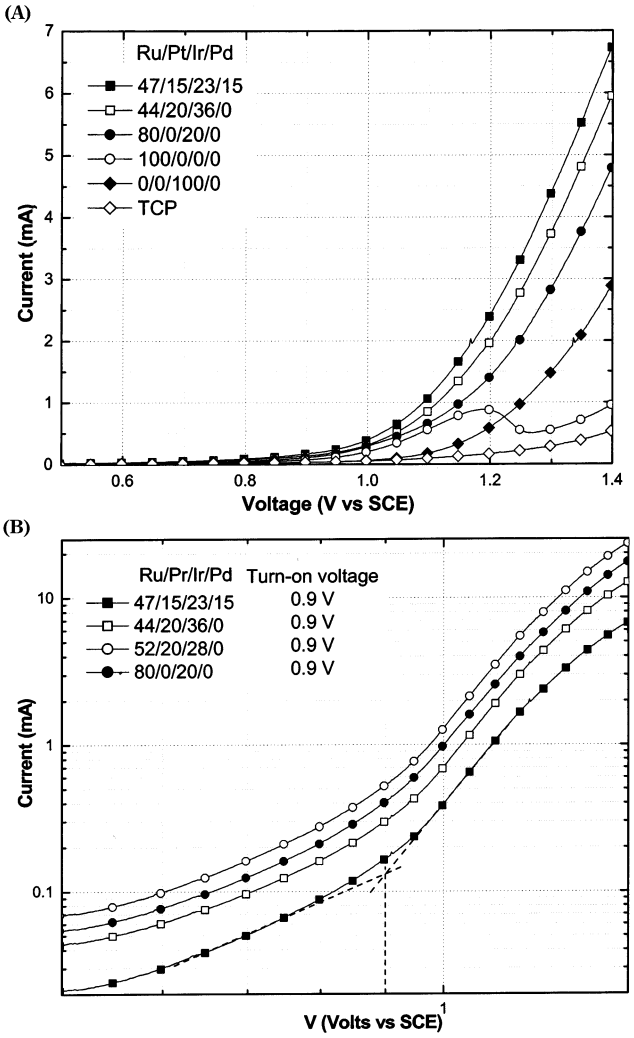

Figure 4. Comparison of *I*−*V* curves of the most active four-, three-, two-element mixtures; Ir; and Ru. The TCP *I*−*V* curve is shown as a reference. The curves of some of these and the other most active microelectrodes are shown on a logarithmic scale in Figure 4B.

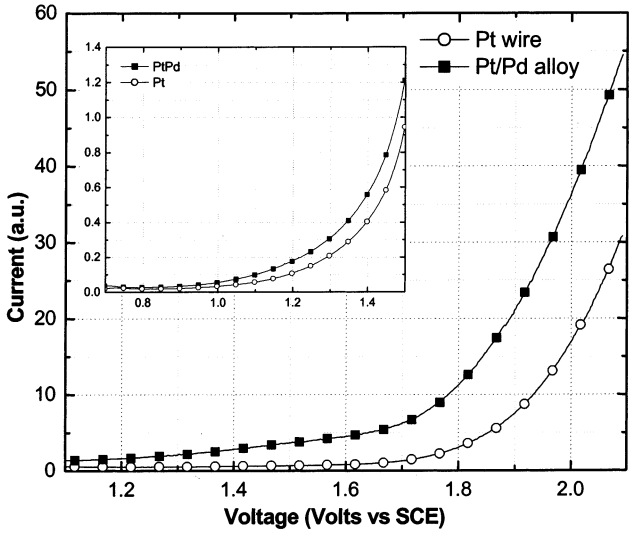

Figure 5. Comparison of electrochemical activity of Pt/Pd (1/1.75 ratio) and pure Pt electrodes. Inset: TCP-supported microelectrodes of the same composition.

Summary

We have examined a large number of supported metal electrodes for water oxidation. The supported electrodes were prepared by the deposition of metal salts onto graphite paper, followed by calcination and hydrogen reduction to give nanoparticulate metals strongly bound to the graphite fibers making up the paper. Ru was the most active single metal as a microelectrode material for the water oxidation reaction. However, it is unstable at higher potentials. Adding Ir, Pt, or Pd to the Ru electrode improves its stability and increases its activity at higher potential. The Ir/Ru electrode exhibits improved performance, relative to electrodes of Ru or Ir alone, at low and high potentials. Improvement in the electrode activity of supported metal microelectrodes can be achieved by moving from individual and binary systems to quaternary mixtures of Ru, Ir, Pt, and Pd. The best combination of metals was found to be $47\%_{atom}$ Ru, $15\%_{atom}$ Pt, $23\%_{atom}$ Ir, and $15\%_{atom}$ Pd.

Acknowledgment. The authors thank the Global Photonic Energy Corporation for their funding of this work. We are very grateful to graduate student Jinglin Yang for PTP fluorescent indicator synthesis. We also appreciate Mr. Jack Worral's advice in SEM/EDX analysis.

CM0117230